Proceedings World Geothermal Congress 2015
Melbourne, Australia, 19-25 April 2015

Seismic Mapping and Geomechanical Analyses of Faults within Deep Hot Granites, a Workflow for Enhanced Geothermal System Projects

H. Abul Khair[1], D. Cooke[1], M. Hand[2]

[1]TRAX, [2]SACGER, University of Adelaide, North Terrace, Adelaide SA 5005

Hani.abulkhair@adelaide.edu.au

Keywords: Enhanced Geothermal System, Seismic, Fault and fracture network, Geomechanics.

ABSTRACT

Areas with deep seated radioactive granites are considered targets for Enhanced Geothermal System (EGS) projects. These areas normally exhibit high heat flow and temperature anomalies related to granitic bodies. High concentrations of uranium within the granites are the most likely cause of the anomalous temperatures. Elevated temperatures are also resulted to high heat flow and thick sedimentary rock cover that includes insulating materials such as coals and gas reservoirs.

In this study we investigated the use of 3D seismic amplitudes and attributes to map deep granitic bodies and faults in the Cooper Basin of South Central Australia. We established a workflow for possible geomechanical fluid flow susceptibility analyses for faults that intersect granites. The far field stress tensor must be interpreted through analyses of image logs and formation tests. Our geomechanical analyses models how this stress tensor affects basement faults interpreted from 3D seismic surveys. Normal stresses, shear stresses, slip tendency, and distance to failure should be modelled for the faults that cut the granites. The optimal orientation of faults that can be possible conduits are then located. We suggest that the optimal injection and production wells should be located at tips of shallow faults that penetrate the granites. We anticipate that short horizontal faults that are located far from other faults will form a more secure fluid conduit. Finally, this study can be a workflow to evaluate the relative merit of future enhanced geothermal system projects.

1. INTRODUCTION

Most geothermal power generating systems are located where naturally occurring hot water and highly permeable rocks are capable of carrying the heat to the surface (Tester, 2006). However, potentially large geothermal energy resources are within reach of conventional drilling techniques in hot, dry and low permeability rocks (HDR) (Tester et al., 2006). The unconventional geothermal reservoirs, which are also called Enhanced Geothermal Systems (EGS) reservoirs, are geothermal systems without natural convection. These systems can be enhanced by pumping water through pre-existing faults and fractures causing them to hydro-shear (Legarth et al., 2005). Thus, success of EGS development requires high heat flows and conductive subsurface corridors, which may include optimally oriented pre-existing, open faults or fractures.

The case study used to establish the workflow for EGS development in the current research is the Cooper Basin in south-central Australia. This is a region of high geothermal gradients and high surface heat flow (Cull and Denham, 1979) (Figure 1 A, B and C). This anomalous area is part of a regional high heat flow anomaly that was attributed by some researchers to the enrichment of radiogenic elements within the Proterozoic basement (e.g. Sass and Lachenbruch, 1979). In contrast, others attributed the anomaly to the Middle Carboniferous high-heat-producing granitic bodies of the Big Lake Suite (BLS) underlying the Cooper Basin sediments (e.g. Beardsmore, 2004). Beardsmore (2004) found that the average vertical heat flow is over 100 mW/m^2 in the Moomba-Big Lake area above the granites and drops significantly beyond the edges of the BLS granites. Meixner et al., (2011), suggested that high mantle heat flows coupled with an insulating sedimentary blanket might also be the reason behind the high temperatures. Meixner et al., (2012) used 3D gravity and magnetic data to model the depth of these granitic bodies and coupled these results with potassium and heat flow measurements to create a thermal map of the Cooper Basin. Many authors propose that the combination of high heat flows and high temperature gradients over the BLS form a potential geothermal energy resource (e.g. Beardsmore, 2004).

A thick clastic sedimentary sequence > 3km covers the BLS in the Cooper Basin, with intercalations of coal beds. This sequence provides good thermal insulation which, combined with the high heat flows and thermal gradients, result in temperatures up to 250 °C at depths 4-5 km (Holgate, 2005). Image logs from wells penetrating the granites in the Moomba area (e.g. Moomba 73), showed fracture densities averaged 0.2 fracture/meter (Abul Khair et al., 2013). Seismic interpretation of the 3D Moomba-Big Lake survey identified more than 300 faults penetrating the basement rocks. Thus, the geothermal system in the Cooper Basin contains all the required elements of high heat flows and high temperature gradients to the faults and fractures needed for EGS development.

The aim of this study is to generate a workflow for EGS projects. It will include the use of: (1) seismic amplitudes and attributes to map the granitic bodies; (2) maps of faults and fractures at the BLS surface; and (3) geomechanical fluid flow susceptibility analyses to model the potential fluid conduits within these rocks.

2. GEOLOGY AND TECTONIC SETTING OF THE COOPER BASIN AREA

Following the deposition of the Cambrian-Ordovician sequences in the Warburton Basin (Figure 2), north west – south east compression caused a partial inversion of the Warburton Basin, deformation of the pre-existing sequence and the subsequent intrusion of Middle to Late Carboniferous granites (Gatehouse et al., 1995). This tectonic event is coeval with the Alice Springs and Kanimblan Orogenies, which affected central Australia and the eastern Australian basins. All published basement seismic interpretations are normally top Warburton sediments or top granites if the granites are present.

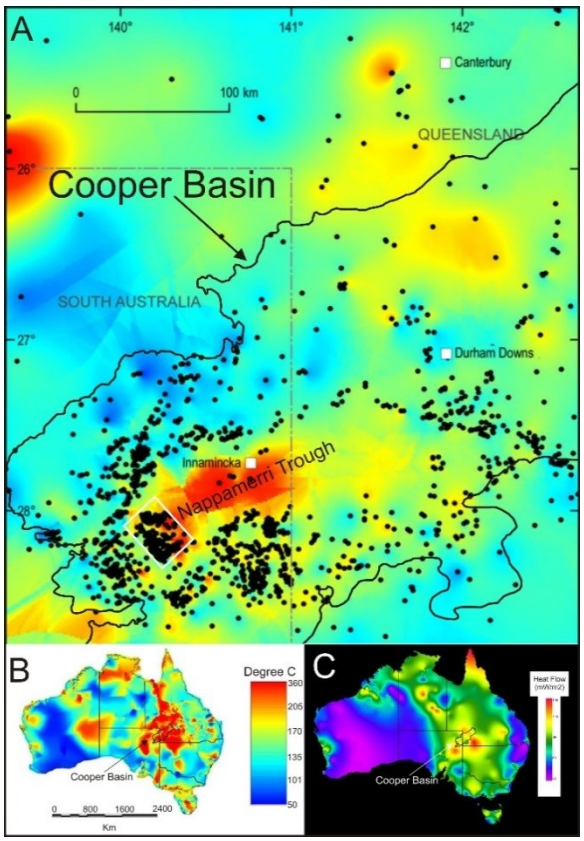

Figure 1: Map of predicted temperatures at 5 km depth in the Cooper Basin (A), and across Australia (B) (Gerner and Hogate, 2010). Color legend in B applies to the main image. Scale bar in B applies to C, Black dots are wells from which temperature measurements were taken. White rectangle represents the location of the 3D seismic survey. Surface heat flow across Australia (C) is also shown (from Hot Dry Rocks Pty Ltd).

The overlying Cooper Basin, is a Late Carboniferous to Middle Triassic basin located in the eastern part of central Australia (Figure 3). The basin is ~2500 m thick and composed mainly of clastic rocks intercalated with coal seams deposited in an environment largely controlled by Gondwanian glaciations (Powell and Veevers, 1987). A basin-wide erosional unconformity marked the end of the Permo-Triassic Cooper Basin caused by the Hunter-Bowen Orogeny (Wiltshire, 1982), which shifted the depocentre northwest and triggered the formation of the Eromanga Basin.

2.1. Geological and structural characterization

The granite cupolas can be identified on seismic sections by a lack of continuous internal reflections and their domal shape (Figure 5). The strong multiples that can sometimes be seen within the granites can confuse interpretation of rock type. Additionally, there is a low sonic and density contrast between the Cooper Basin deposits and the basement rocks leading to a weak contrast in the seismic signal. Due to the low contrast in density and seismic velocity between Cooper Basin and Warburton Basin rocks, there is a low acoustic impedance contrast. Another challenge for defining the basement is the existence of granitic wash above the fresh granites. Boucher (1997) interpreted it as BLS in most of the wells.

2.2. Thermal characterization

Vertical heat flow is commonly greater than 100mW/m2 in the wells overlying the granitic bodies, while low heat flow (25 W/m2) is observed above Warburton Basin sedimentary deposits (Beardsmore, 2004). The highest vertical heat flow measured was in Moomba 139, which lies adjacent to a granitic body. Beardsmore (2004) related the elevated heat flow over a non-granitic basement as due to possible roof pendant at the top of a thick granitic body. The seismic data shows no granites indicating that granitic basement is deeply seated under well Moomba 139. However, the well is located above a fault that penetrates all the underlying rocks including the granites (Figure 5). This suggests that the vertical high heat flow in this well and similar wells is possibly related to heat transfer through thermally conductive, deeply seated faults that are directly connected to granitic bodies.

Thermal conductivity for the different formations was estimated by Beardsmore (2004) and later by Meixner et al. (2012). The Patchawarra and Toolachee Formations show the lowest thermal conductivities (Table 1). The Patchawarra Formation consists of approximately 6% coal seams, and coal has a considerably lower thermal conductivity (~0.3 W/mK) than most rocks (2–5 W/mK) (Beardsmore, 2004). Also, the Patchawarra and Toolachee formations frequently contain insulating gas reservoirs. Gas filled rock is a thermal insulator and tends to reduce thermal conductivity of a formation by 25%. Beardsmore (2004) found that gas reduced heat the flow by up to 5% in Big Lake 33. Finally, thermal conductivity of rock decreases with increasing temperature, causing hot Patchawarra and Toolachee formations to insulate the deeper granites.

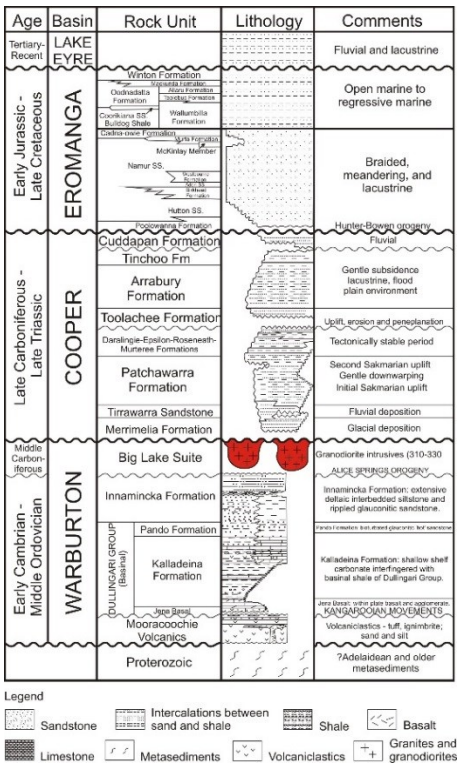

Figure 2: Geological summary of the Cooper region (modified after Cotton et al., 2006). The red color represents the granitic intrusion of heat source in the Cooper Basin.

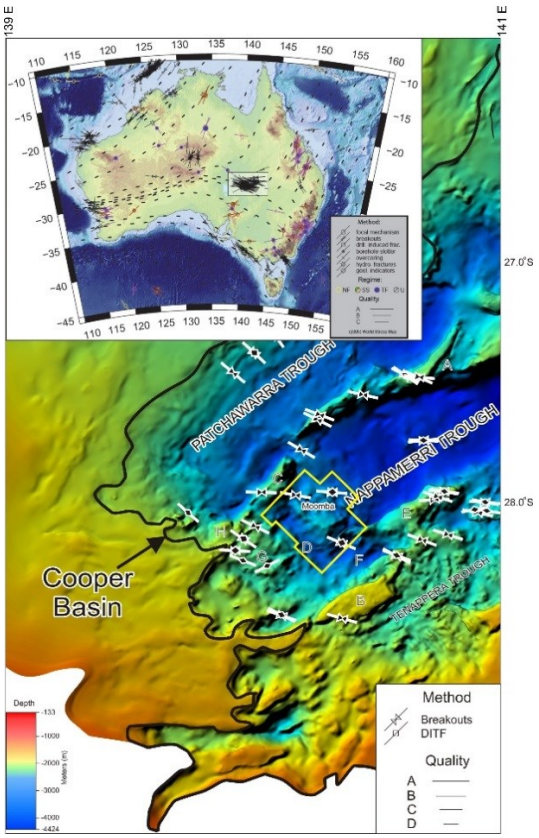

Figure 3. Top Warburton Basin (Pre-Permian Basement, seismic horizon Z) in the Cooper Basin (Modified after NGMA, 2009). Map shows NE - SW major troughs separated by ridges. Study area is located at the southwestern termination of the Nappamerri trough (Moomba-Big Lake 3D seismic cube outlined in yellow). A: Innamincka Ridge; B: Murteree Ridge; C: Gidgealpa - Merrimelia Ridge; Wooloo Trough; E: Della-Nappacoongee Ridge; F: Allunga Trough; H: Warra Ridge. Top left: Australian stress map (Modified after Hillis and Reynolds, 2000 and Heidbach et al., 2010), SH indicated in black lines.

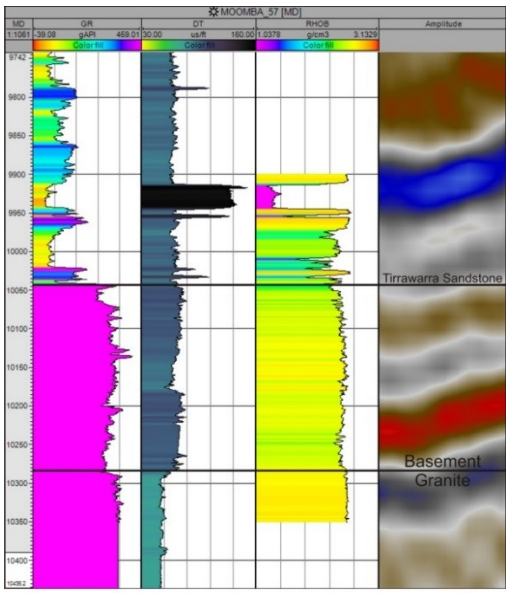

Figure 4: Well log comparison of the Tirrawarra Formation and basement rocks (sedimentary deposits or granites) in Moomba 57. The similar gamma-ray signature between the Tirrawarra Formation and the granites is due to Tirrawara Formation deposits being sourced from the granites. Variations in density and sonic velocity within the basement indicate a sedimentary basement rather than granitic basement.

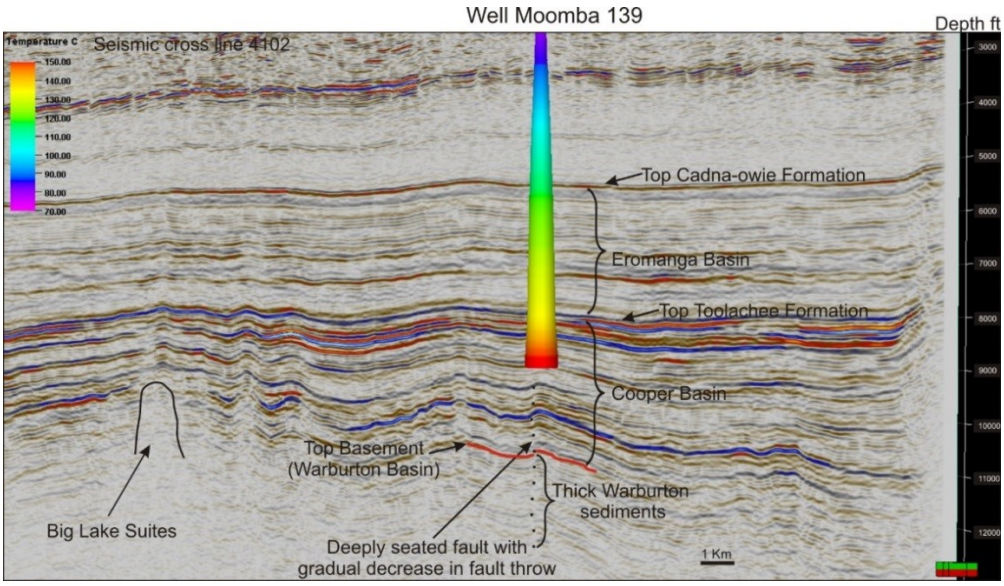

Figure 5: Well Moomba 139 displayed against seismic cross line 4102 in the Moomba-Big Lake cube. The well contains the highest heat flow in the field, probably due to overlying a deeply seated fault.

Table 1: Average thermal conductivity measurements for some of the Cooper and Warburton Basins in the Moomba Big Lake area.

ROCK UNIT	MEAN THERMAL CONDUCTIVITY (W/mK) (Meixner et al., 2012)	STANDARD DEVIATION (W/mK) (Meixner et al., 2012)	THERMAL CONDUCTIVITY (W/mK) (Beardsmore, 2004)
Surficial	3.31	0.51	2.3 ±0.23
Hutton	4.10	0.65	5.0 ±0.84
Toolachee	1.63	0.46	1.29 ±0.36
Patchawarra	2.10	0.66	1.61 ±0.31
Tirrawarra	2.99	0.51	3.7 ±0.56
Basement (none granitic)	3.54	0.89	4.13 ±0.49
Granite	2.79	0.38	0.61

3. DATA AND METHODOLOGY

This study focuses on the Moomba-Big Lake fields, which are located at the south-western termination of the Nappamerri Trough in the Cooper Basin (Figure 3). The fields are covered by a 3D seismic reflection survey with an area of ~800 km2 and contain around 300 oil and gas wells. Of these wells, twenty-nine wells have check shots that allow the seismic data interpretation to be tied to the geology. Recorded data in most of the wells include wireline logs, drill stem tests (DST), repeated formation tests (RFT), leak off tests (LOT), and hydraulic fracture tests. Image logs are available from seven wells, which are providing images of the sediments and the granites.

The top of the Warburton Basin was picked on the 3D seismic data and the granitic bodies, which are referred to as granitic cupolas, were mapped using seismic amplitudes. Structural interpretation of seismic amplitudes and attributes has led to the identification of large-scale faults and fracture networks within the basement granites. A geomechanical fluid flow susceptibility (GFFS) model was constructed for the faults that cut the granites after calculating the in-situ stresses. The GFFS model will help locate faults that are optimally oriented and could provide permeable corridors for hot water circulation. The GFFS analyses consists of calculating the pore pressure and orientation and magnitude of the in-situ stresses, defining the granitic bodies using seismic amplitudes, interpreting deep faults penetrating the granites, and modelling normal and shear stress, dilation tendency and distance to failure for every fault.

For more details about pore pressures calculation and the stress tensor please refer to Abul Khair et al (2015)

4. IN-SITU STRESS MAGNITUDES AND ORIENTATION

Our analyses of the interpreted 104 breakouts and 29 drilling induced tensile fractures show a consistent SH direction trending at N101˚ E (Table 2). This is consistent with a previous basin-wide study conducted by Reynolds et al., (2004), which gave a SH orientation of N 101˚, as interpreted from compiled data across the entire of the Cooper Basin.

Table 2: Number of borehole breakouts and drilling-induced tensile fractures recorded in each well.

Borehole name	n	Total length (m)	SH orientation	S.D.	Quality[a]
Big Lake 54	67	64	104°N	5.5°	B
Moomba 73	31	35	97°N	6.5°	C
Moomba 74	7	11	101°N	3°	D
Moomba 78	28	42	97°N	5.3°	B

a: Data quality ranking according to the World Stress Map (Heidbach et al., 2010)

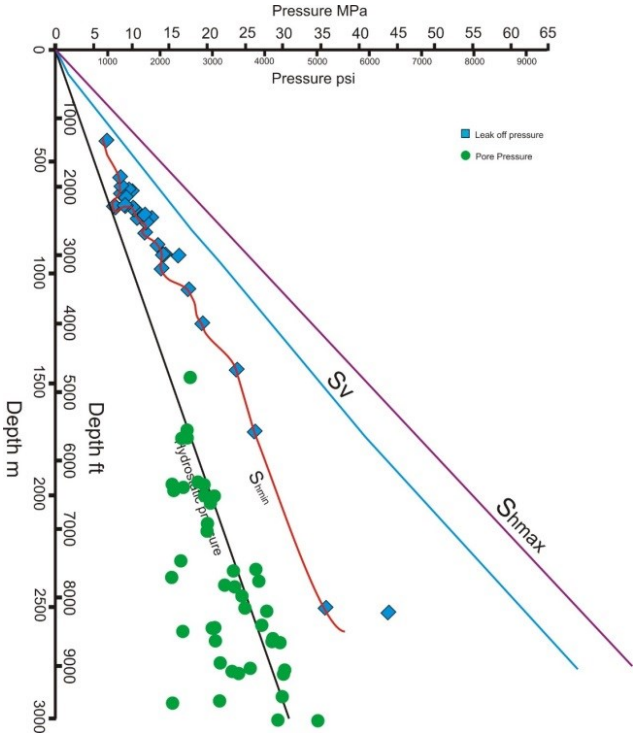

Figure 6: Stress magnitude verse depth plot of the Moomba - Big Lake field. Sv: vertical stress, SH: maximum horizontal stress, Sh: minimum horizontal stress.

The calculated magnitudes of the three principal stresses in the Moomba-Big Lake fields showed that SH is the maximum principal stress and the magnitude of the vertical stress is greater than the minimum horizontal stress. Thus, a strike-slip stress regime (SH > Sv > Sh) dominates the field (Figure 6). This result is consistent with the results of Reynolds et al. (2004), who showed that the stress regime changes with depth to a reverse fault stress regime. The current study didn't show this change as the available data do not cover deep intervals compared with other parts of the basin.

5. MAPPING THE GRANITES AND THEIR FAULTS

5.1. Seismic reflection data

More than 500 faults were mapped based on the 3D seismic data with the majority trending east-northeast (Figure 7 and 8). A less dominant trend of northwest can also be seen. Most of the faults cut the basement, but very few reach the top of Patchawarra Formation in the Cooper Basin. A gradual upward decrease in the fault throw was recognized indicating rejuvenation during Triassic tectonic activity (Figure 5). Some of these faults cut the Warburton sedimentary deposits, while others are located within the granites.

The top of Warburton Basin interpreted horizon demarcates the upper limit of either the Warburton sediments or Big Lake Suite granites (Figure 5 and 7). The interpreted basement is dominated by fault propagation antiforms. Most of the faults related to the granites bound the granitic cupolas, with few located within the granitic cupolas. This suggests that the intrusion of the granites in the Middle Carboniferous might be controlled by pre-existing faults, or that intrusion of granites generated planes of weakness at the boundaries with the host rocks, which then developed into faults during uplift (Figure 9). The granitic cupolas can be distinguished within the seismic sections through their general domal geometry and their lack of continuous internal seismic reflections. Meixner et al. (2012) modelled the distribution of the granitic bodies using regional magnetic and gravity data. They modelled granites in the Cooper Basin area using gravity inversion and measured density from well logs (Figure 10).

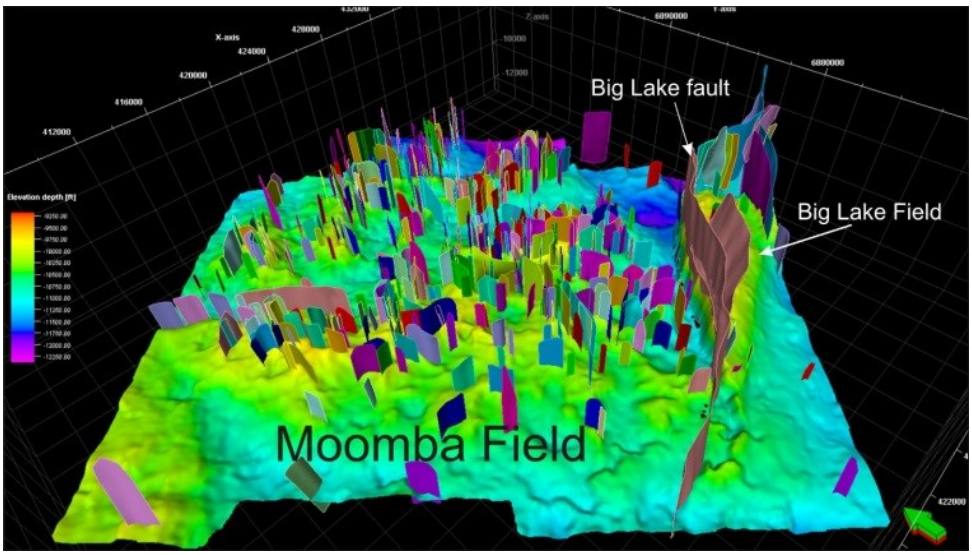

Figure 7: Top of Warburton basement in the Moomba-Big Lake fields showing all the faults penetrating the basement rocks including the major Big Lake fault that separates the Moomba field from the Big Lake field. The depth colour key will be used for the figures 14-19.

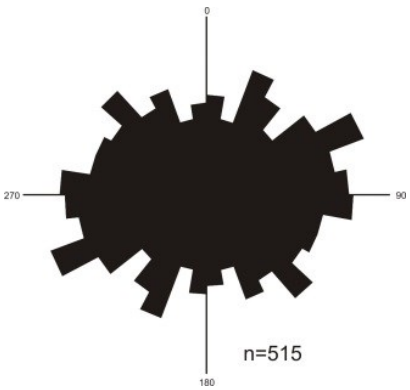

Figure 8: Rose diagram of the faults interpreted from the seismic data within the Moomba-Big Lake seismic volume. A east-northeast trend can be seen.

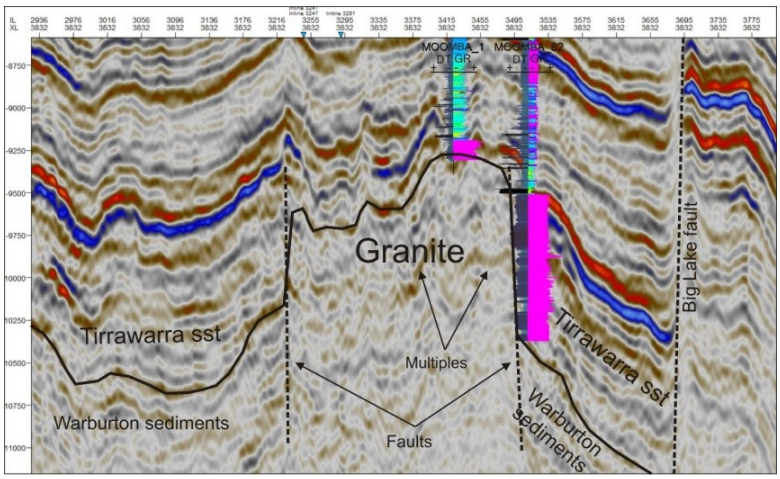

Figure 9: Seismic crossline 3832 showing the top of the Warburton basement (solid black line) underlain by sedimentary rocks (to the right and left of the faults). Wells displays gamma-ray (to the right) and sonic velocity (to the left). Moomba-82 didn't penetrate granite although it does show high gamma-ray values, whereas Moomba-1 penetrated granites. Some multiples can be seen within the granites.

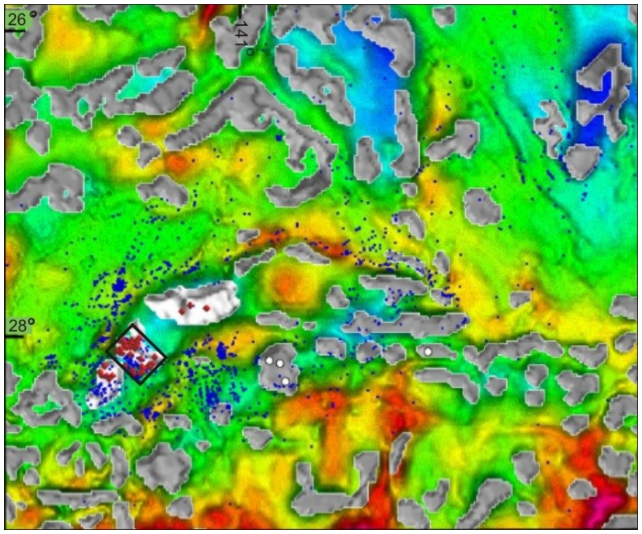

Figure 10: Set of granitic bodies created from the gravity inversion density model (grey-granites; white-granodiorite) draped over a gravity image. Red dots are wells that intersect granodiorites, white dots are wells intersecting granites; and blue dots are the locations of the temperature measurements. The white box shows the location of the Moomba-Big Lake fields (Modified after Meixner et al., 2012).

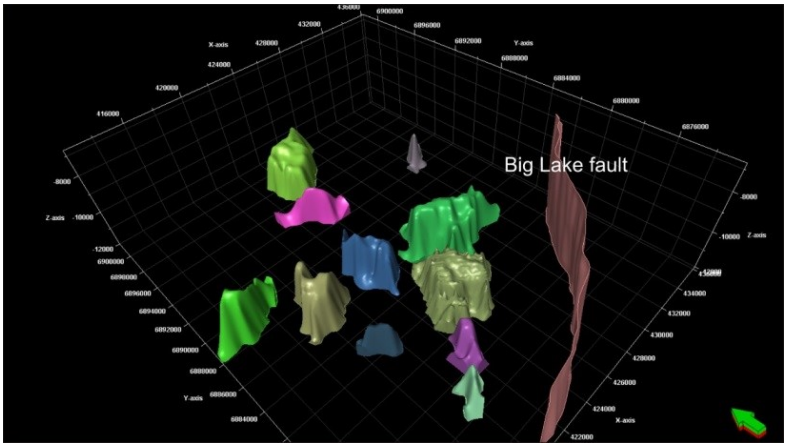

Figure 11: Places in the Moomba field where the granitic cupolas intrude the interface beneath the Cooper Basin deposits. The large fault to the right is the Big Lake fault.

5.2. Seismic attributes

We used curvature attributes in our structural interpretation. Curvature is defined as the reciprocal of the radius of a circle that is tangent to the given curve at a point (Figure 12) (Chopra and Marfurt, 2007). An observed high value of curvature corresponds to a curve; whereas curvature will be zero for a straight line (the same concept is applicable to surfaces). Curvature was used to validate the fault interpretation and to locate possible highly fractured areas.

6. GFFS

Our principal aim is to locate the faults and fractures that are most likely to conduct fluids. In the current study, we interpreted approximately 170 faults from seismic amplitudes and attributes that intersect the granites (Figure 13). Stresses calculated in the current study were applied to the faults to determine which are optimally oriented.

Our geomechanical model subjected the interpreted faults to a far field stress gradient of 1.216 psi/ft (27.5 MPa/km), 0.6898 psi/ft (15.6 MPa/km), and 1.0126 psi/ft (22.9 MPa/km), for the maximum horizontal stress, minimum horizontal stress, and vertical stress, respectively with a pore pressure gradient of 0.44 psi/ft (10 MPa/km). The maximum horizontal stress direction used in the model was 102°, fault cohesion was 0.6, and the friction angle was 15°. Normal and shear stresses, slip tendency, and distance to failure were all calculated for every fault to determine which are optimally oriented.

6.1. Normal stress is the stress oriented perpendicular to the fault surface. It is calculated from the equation:

$$\sigma n = \left\{\frac{\sigma 1 + \sigma 3}{2}\right\} + \left\{\frac{\sigma 1 - \sigma 3}{2}\right\} \cos 2\theta \quad (1)$$

Where σn is the normal stress, σ1 is the maximum horizontal stress, σ3 is the minimum horizontal stress, and Θ is the angle between the stress vector and the fault surface. Normal stresses act against the opening of the fault and thus reduce fluid circulation. As the maximum horizontal stress is oriented at 101°, faults trending at 012° are subjected to high normal stresses 3000-4000 psi (20.7-27.6 MPa). As the fault deviates further from this direction, normal stresses applied on the fault surface decrease allowing it to be conduits (Figure 14).

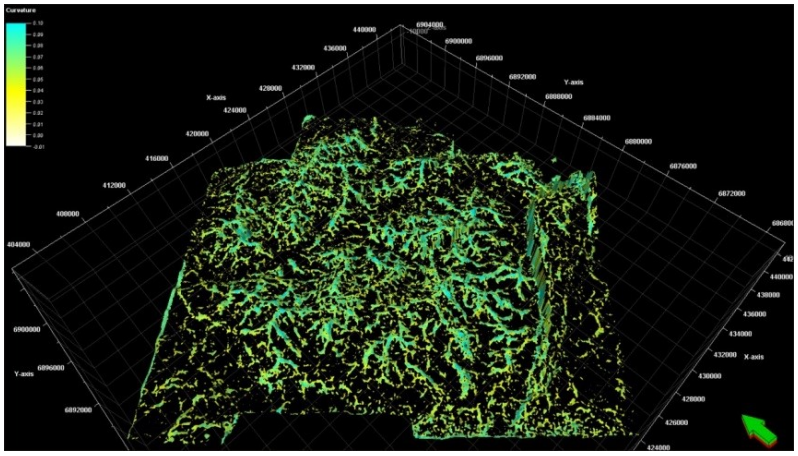

Figure 12: Most positive curvature attribute displayed on top of the basement horizon showing the fault and highly curved locations network.

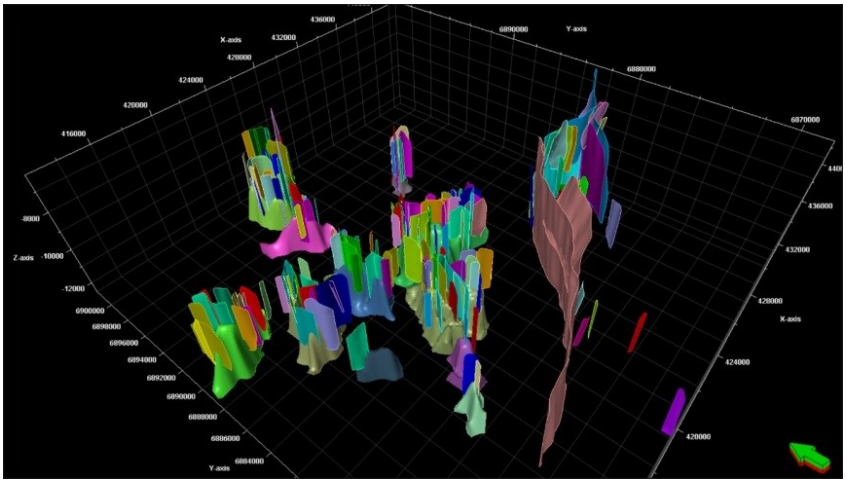

Figure 13: Faults cutting the granitic cupolas in the Moomba area displayed on the top of the granitic bodies.

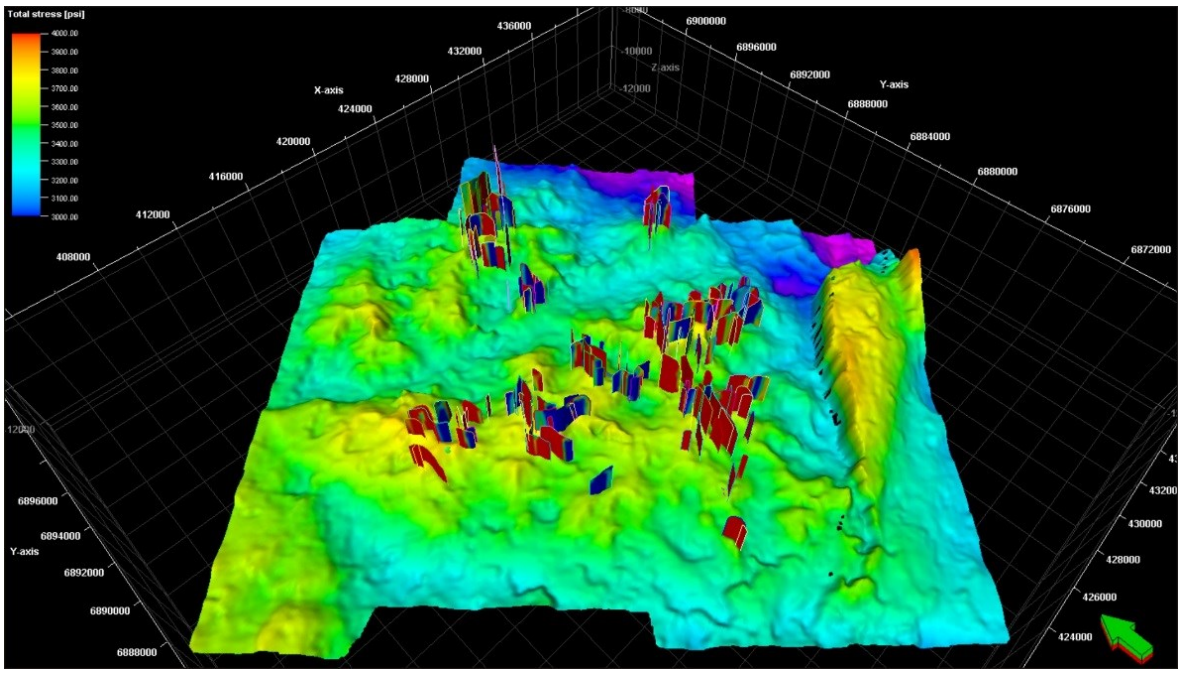

Figure 14: Faults penetrating the granitic cupolas in the Moomba-Big Lake fields displayed at the top of the interpreted basement. Colours displayed on the faults are normal stress attributes calculated from the far field stress. 1000 psi = 6.9 MPa.

Shear stress is the stress vector that acts parallel to the fault surface. Shear stress is calculated from the equation:

$$\sigma s = \left\{\frac{\sigma 1 - \sigma 3}{2}\right\} \sin 2\theta \qquad (2)$$

Where σs is the shear stress. Optimally oriented faults are subject to shear stresses up to 2500 psi (17.2 MPa). Whereas faults with orientations that are close to perpendicular to the maximum horizontal stress are subject to low shear stresses (less than 1500 psi, or 10.3 MPa) (Figure 15). While pumping the fluids in the injection well, hydraulic shearing will most likely occur along the fault, and a permeable corridor along the fault plane will enhance circulation. As the shear stress applied to the fault planes increases, mobility of hydro-shearing also increases.

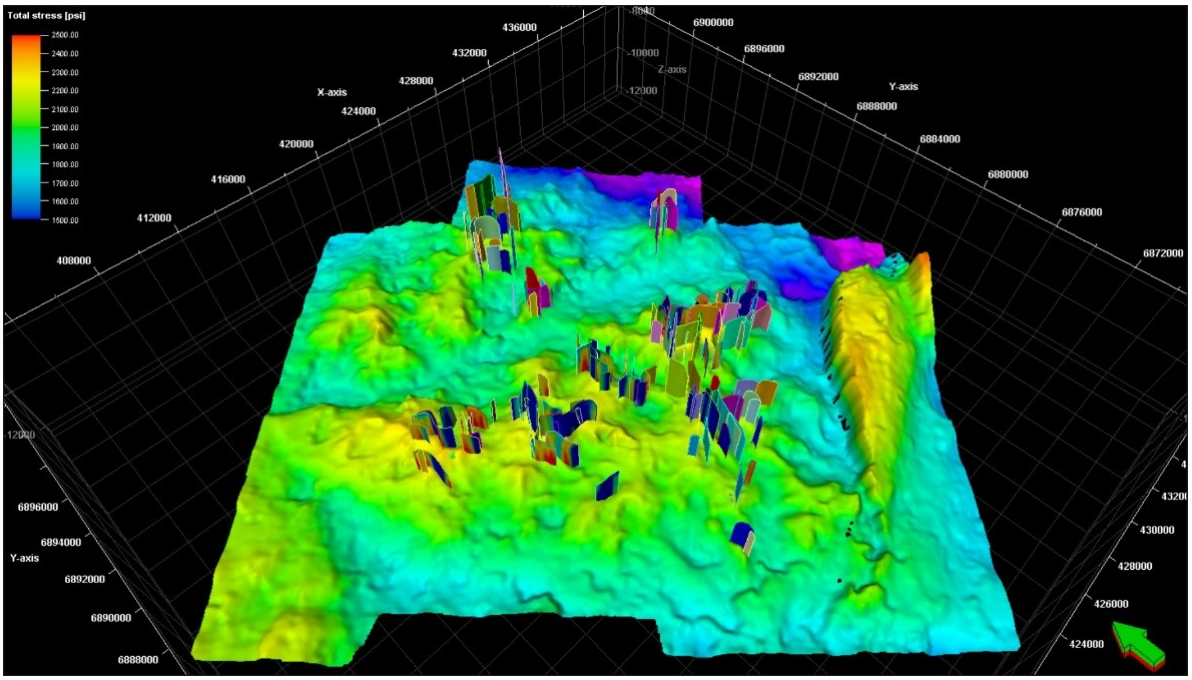

Figure 15: Faults penetrating the granitic cupolas in the Moomba-Big Lake fields displayed at the top of the interpreted basement. Colors displayed on the faults are shear stress attributes calculated from the far field stress. 1000 psi = 6.9 MPa.

Slip tendency is a predictor of both the likelihood and the direction of slip on the fault surface (Morris et al., 1996). Slip tendency (Ts) of a fault is defined as the ratio of the shear stress to the normal stress on the fault surface:

$$Ts=\sigma s/\sigma n \quad (3)$$

The calculation of *Ts* is based on the fact that the resolved shear and normal stresses can predict slip along the fault. Faults with a high slip tendency orientations are better flow conduits than faults with a low slip tendency orientation (Barton et al., 1995; Morris et al., 1996). The preferred fluid flow through fault pathway is more when the differential stress (σ1-σ3) is greater and the area of the fault experiencing high tendency is greater (Morris et al., 1996) (Figure 16).

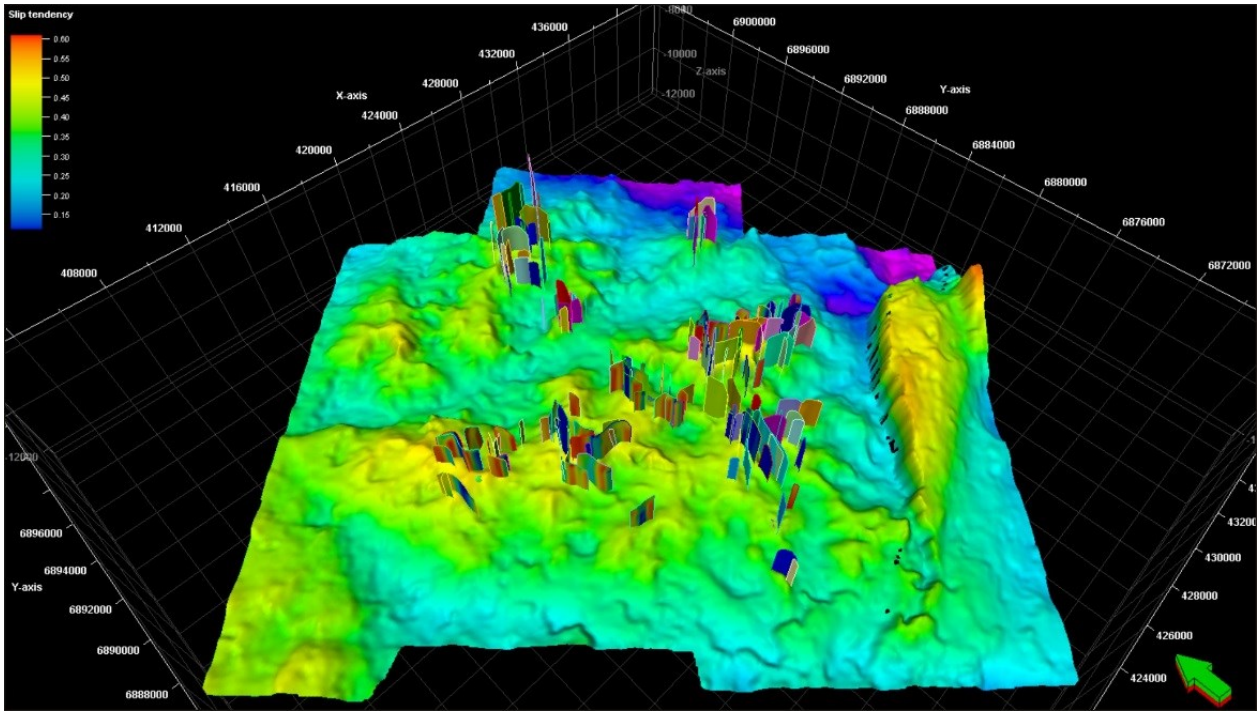

Figure 16: Faults penetrating the granitic cupolas in the Moomba-Big Lake fields displayed at the top of the interpreted basement. Colours displayed on the faults are slip tendency attributes calculated from the far field stress.

Distance to failure, which is sometimes called fault susceptibility, requires a detailed knowledge of the in-situ stress field and fault orientations (Reynolds et al., 2004). Faults that are optimally oriented for reactivation within the in-situ stress field will have higher permeability than faults that are not (Barton et al., 1995). The horizontal distance between each point at the fault plane and the failure envelope represents the pressure increase required to initiate failure (Figure 17 and 18). By applying this technique, fault reactivation estimates can be made and thus the susceptibility of the faults to fluid flow.

We applied the calculated stresses on the faults considering a fault failure envelope with cohesive strength of 0.6 and angle of friction of 15 °. The results showed some of the faults are critically stressed (i.e. low stress needed to initiate failure). Whereas, some faults show a total stress of 1000 psi (6.9 MPa) needed to initiate failure (Figure 17).

7. DISCUSSION

Several factors must be considered when studying unconventional geothermal project sites. First, the source of heat should be within the depth target of conventional petroleum drilled wells. This will help maintain water circulation which will be controlled using suitable well completions. Geothermal gradients and heat flows should be modelled to locate thermal sweet spots. Thermal conductivity is a potential factor that controls heat preservation in the subsurface. Horizons of low thermal conductivity such as coal seams and gas reservoirs, if present within the sequence, should be targeted for possible heat insulation.

The second important approach that has proven to be important in unconventional geothermal projects is the use of 3D seismic amplitudes and attributes to map the heat sources (granites in this study), and the faults that intersect them. A 3D structural model should be built for the heat source and the faults. Geomechanical fluid flow susceptibility analyses must be conducted to locate potential faults. This requires the calculation of the orientations and magnitudes of the principle stresses in the target region and modelling these stresses at the fault planes.

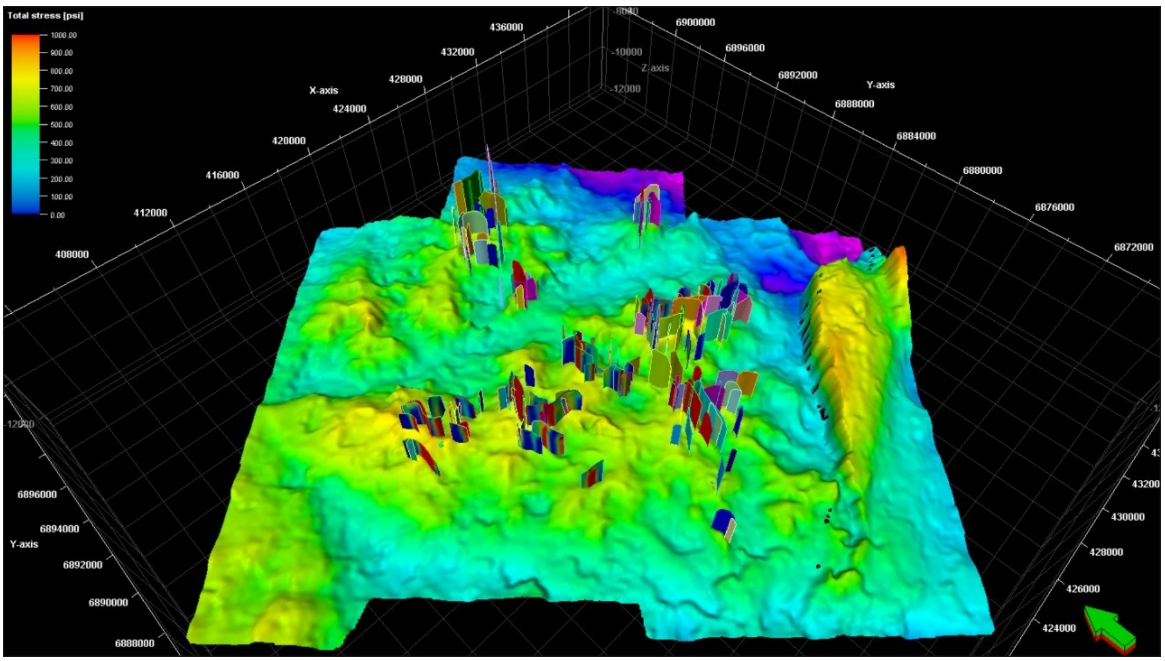

Figure 17: Faults penetrating the granitic cupolas in the Moomba-Big Lake fields displayed at the top of the interpreted basement. Colors displayed on the faults the distance to failure attributes calculated from the far field stress. 1000 psi = 6.9 MPa.

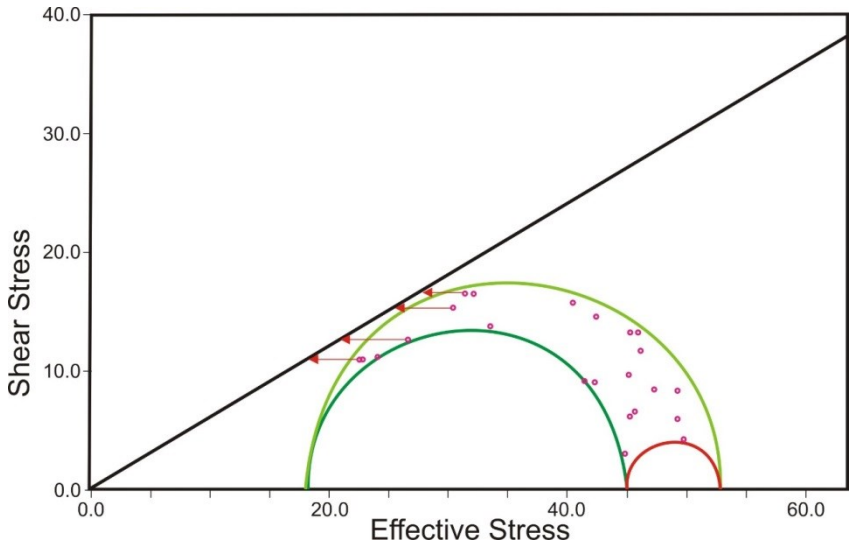

Figure 18: Mohr diagram for well Moomba 78 at a depth close to the top of the granites showing how far the fractures in the subsurface are from reactivation.

The faults that are the best potential conduits for fluid circulation in a geothermal project are those that are optimally oriented. Optimally oriented faults will be characterized by low normal stress, high shear stress and slip tendency, and undergo failure at low pressures. In this study, we considered the threshold for potential faults using the calculated stresses are the values that require less pressure for stimulation and are as follows:

- Normal stress = less than 27.6 MPa.
- Shear stress = more than 13.8 MPa.
- Slip tendency = of more than 0.4 are considered potential faults.
- Distance to failure = faults that require less than 3.5 MPa to be reactivated are considered potential conduits.

Comparing stresses calculated on the faults that intersect the granitic bodies in the Moomba-Big Lake area using the above thresholds, 9 faults exhibit the required characteristics (Figure 19). Further ranking of these faults should depend on the length of the fault, depth of the fault, and how close the fault is to neighboring faults. As the horizontal extension of the fault decreases, this helps constraining the water circulation within a limited distance and prevents circulation loss. Also, shallow penetrating faults in

the granites (not cutting to high depths), risk less water loss during circulation. Finally, the closer a fault is to a neighbouring fault, the higher the risk of break through and the loss of the injected water during water pumping.

8. CONCLUSIONS

The current paper represents a workflow that helps locate potential sites for enhanced geothermal system projects. The work flow is summarized as follows:

- Conduct acquisition and processing of 3D seismic data which should be designed to optimize the image of the basement/heat sources and faults.
- Map the basement reflector and the faults penetrating it.
- Calculate the most positive curvature attribute on top of the basement horizon and validate the fault interpretation.
- Interpret image logs and determine stress orientations.
- Calculate/measure pore pressures, vertical stresses, minimum horizontal, and maximum horizontal stresses using direct measurements and calculations (refer to text) if direct measurements are not available.
- Perform the geomechanical fluid flow susceptibility analyses to identify the optimally oriented faults.
- Rank faults based on calculated stresses and on vertical and horizontal extent and distance from other faults.
- Plan the injection and production wells to be at tips of the potential faults. This will constrain water circulation within the fault plan and will prevent any water loss.

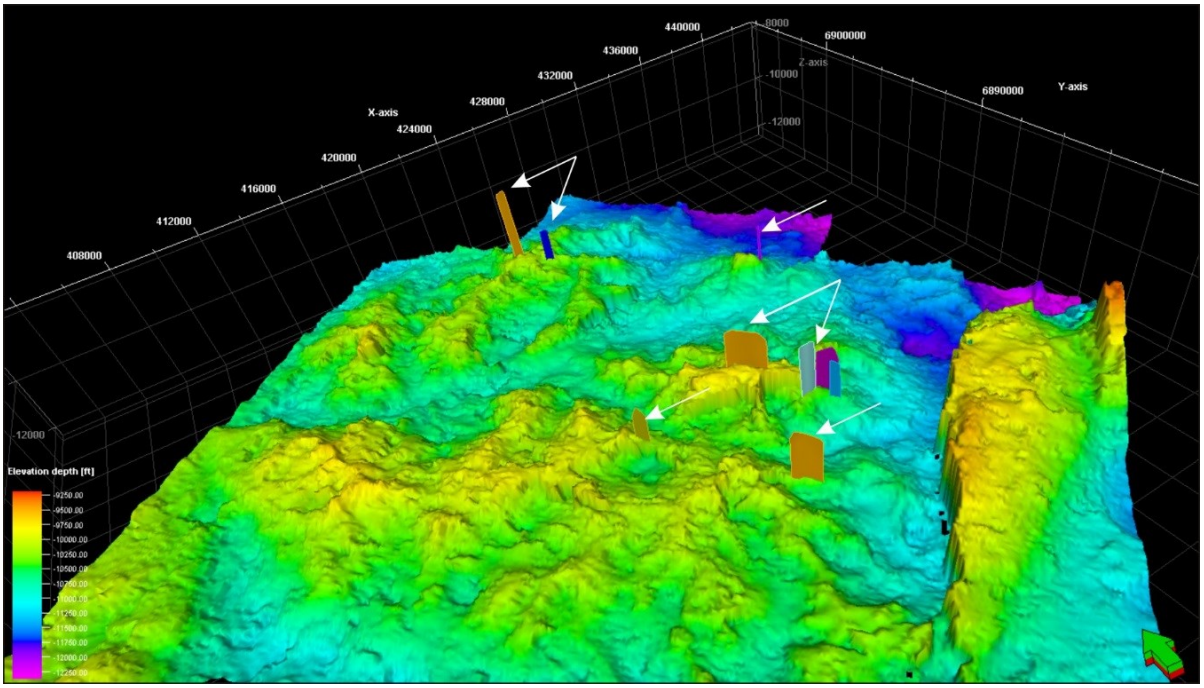

Figure 19: Optimally oriented faults (indicated by white arrows) in the Moomba-Big Lake area displayed on top of the basement.

ACKNOWLEDGEMENTS

The authors really appreciate and thank Geothermics/Elsevier for allowing re-publishing and presenting this paper in the World Geothermal Congress 2015. The authors would like to acknowledge the appreciated financial contribution and provision of the data from the Petroleum and Geothermal division of *The Department for Manufacturing, Innovation, Trade, Resources and Energy (DMITRE)* / PACE 2020: Plan for accelerating exploration. Also, we would like to acknowledge the financial support of *The South Australian Centre for Geothermal Energy Research (SACGER)*. Many thanks to the generous donation of Academic Licenses of Petrel from Schlumberger and JRS Image Log Interpretation Suite from JRS Petroleum Research.

REFERENCES

Abul Khair, H., Backé G., King R. Holford S., Tingay, M., Cooke, D., Hand, M.: Factors influencing fractures networks within Permian shale intervals in the Cooper Basin, South Australia. APPEA, 52, (2012a), 213-228.

Abul Khair, H., Cooke, D., Hand, M.,: The effect of present day in-situ stresses and paleo-stresses on locating sweet spots in unconventional reservoirs, case study from Moomba-Big Lake fields, Cooper Basin, South Australia, Journal of Petroleum Exploration and Production Technology 3, (2013), :207-221.

Abul Khair, H., Cooke, D., King, R., Hand, M., Tingay, M.: Preliminary Workflow for Subsurface Fracture Mapping Using 3d Seismic Surveys. A Case Study from the Cooper Basin, South Australia. Geothermal Research Council conference, Reno-Nevada (2012).

Backé G., Abul Khair H., King R. Holford S.: Fracture mapping and modelling in shale-gas target in the Cooper basin, South Australia, APPEA, 51, (2011), 397-410

Barton, C. A., Zoback, M. D. Moos, D.: Fluid flow along potentially active faults in crystalline rock, Geology, 23 (8), (1995), pp. 683–686.

Beardsmore, G.: The influence of basement on surface heat flow in the Cooper Basin. Exploration Geophysics, 30, (2004), 223-235.

Boucher, R.K.: A Beginner's Guide to Picking Basement from Wireline Logs, Cooper Basin Area. Report book 97/37a, Primary Industries and Resources SA (1997).

Chopra, S., Marfurt, K.: Seismic Attributes for prospect identification and reservoir characterization. SEG geophysical development series No. 11, p 464, (2007).

Cotton, T.B., Scardigno, M.F., Hibburt, J.E.: The Petroleum Geology of South Australia. Vol. 2 and 4, Department for Manufacturing Innovation, Trade, Resources and Energy (2006).

Cull, J.P., Denham, D.: Regional variations in Australian heat flow. Bureau of Mineral Resources, Journal of Australian Geology and Geophysics, 4, (1979), 1-13.

Gardner, G.H.F., Gardner, L.W., Gregory, A.R.: Formation velocity and density – The diagnostic basis for stratigraphic traps: Geophysics, 39, (1974), 770-780.

Gatehouse, C.G., Fanning, C.M., Flint, R.B.: "Geochronology of the Big Lake Suite, Warburton Basin, northeastern South Australia". South Australia. Geological Survey. Quarterly Geological Notes, 128, (1995), 8-16.

Gerner, E., Holgate, F.: OzTemp – Interpreted Temperature at 5 km Depth. Geoscience Australia, Canberra, (2010).

Heidbach, O., Tingay, M.R.P., Barth, A., Reinecker, J., Kurfeβ, D., Müller, B.: Global crustal stress pattern based on the 2008 World Stress Map database release. Tectonophysics 482, (2010), 3–15.

Hillis, R.R., Reynolds, S.D.: The Australian Stress Map. Journal Geological Society of London, 157, (2000), 915-921.

Holgate, F.: Exploration and Evaluation of the Australian Geothermal Resource. PhD thesis, Australian National University, (2005).

Legarth, B., Huenges, E., Zimmermann, G.: Hydraulic fracturing in a sedimentary geothermal reservoir: results and implications. International Journal of Rock Mechanics and Mining Sciences, 42 (7-8 SPEC. ISS.), (2005), pp. 1028-1041

Meixner, A.J., Kirkby, A., Champion, D.C., Weber, R., Connolly, D., Gerner, E.: Geothermal Systems, in: Huston, D. L. and van der Wielan, S. E. (eds). An assessment of the uranium and geothermal prospectivity of east-central South Australia. Record 2011/34. Geoscience Australia: Canberra, (2011).

Meixner, A.J., Kirkby, A.L., Lescinsky, D.T., Horspool, N.: The Cooper Basin 3D Map Version 2: Thermal Modelling and Temperature Uncertinity. Record 2012/60. Geoscience Australia: Canberra, (2012).

Morris, A.P., Ferrill, D.A., Henderson, D.B.: Slip tendency and fault reactivation. Geology 24, (1996), 275–278.

Powell, C.M., Veevers, J.J.: "Namurian uplift in Australia and South America triggered the main Gondwanan glaciation". Nature, 326, (1987), 177-179.

Reynolds, S.D., Mildren, S.D., Hillis, R.R., Meyer, J.J.: The in situ stress field of the Cooper Basin and its implications for hot dry rock geothermal energy development: PESA Eastern Australian Basins Symposium II, p. 431-440, (2004).

Sass, J.H., Lachenbruch, A.H.: Thermal regime of the Australian Continental Crust, in: M. W. McElhinny (ed.) The Earth: its origin, structure and evolution. Academic Press: London, pp 301-351, (1979).

Somerville, M., Wyborn, D., Chopra, P., Rahman, S., Estrella, D., van der Meulen, T.: Hot dry rock feasibility study. Report 94/243. Energy Research and Development Corporation. 133pp, (1994).

Tester, J.: The Future of Geothermal Energy – Impact of Enhanced Geothermal Systems (EGS) on the United States in the 21st Century. Idaho Falls: Idaho National Laboratory.ISBN 0-615-13438-6, (2006).

Wiltshire, M.J.: "Late Triassic and Early Jurassic sedimentation in the Great Artesian Basin". In: Moore, P.S. and Mount, T.J. (Compilers), Eromanga Basin Symposium, Adelaide, 1982. Summary papers. Petroleum Exploration Society of Australia, Geological Society of Australia (SA Branches), (1982), pp.58-67.